ACADEMIC PRESS

Available online at www.sciencedirect.com

SCIENCE DIRECT®

Journal of Sound and Vibration 266 (2003) 993–1008

JOURNAL OF SOUND AND VIBRATION

www.elsevier.com/locate/jsvi

Finite element simulation of non-linear acoustic generation in a horn loudspeaker

T. Tsuchiya*, Y. Kagawa, M. Doi[1], T. Tsuji[2]

Department of Electronics and Information Systems, Akita Prefectural University, 84-4 Tsuchiya-Ebinokuchi, Honjo, Akita 015-0055, Japan

Received 4 February 2002; accepted 4 October 2002

Abstract

The loudspeaker is an electro-acoustic device for sound reproduction which requires the distortion as small as possible. The distortion may arise from the magnetic non-linearity of the york, the uneven magnetic field distribution, the mechanical non-linearity at the diaphragm suspension and the acoustic non-linearity due to the high sound pressure and velocity in the duct-radiation system. A horn is sometimes provided in front of the vibrating diaphragm radiator, which plays an important role to increase the efficiency by matching the acoustic impedance between the radiator and the ambient medium. The horn is in many cases folded twice or three times to shorten the length, which further degrades the reproduction quality. The sound intensity and velocity are apt to attain very high in the small cross-sectional area in the throat and in the folded regions, which may cause the distortion due to the non-linear effect of the medium. The present paper is to investigate the frequency characteristics of the loudspeaker numerically evaluating the generation of the harmonics and sub-harmonics. An axisymmetric folded horn is considered for which the wave equation with the non-linear term retained is solved by the finite element method. The solution is made in time domain in which the sound pressure calculated at the opening end of the horn is Fourier-transformed to the frequency domain to evaluate the distortion, while the wave marching in the horn is visualized.

*Corresponding author. Tel.: +81-184-27-2093.

E-mail address: tsuchiya@akita-pu.ac.jp (T. Tsuchiya).

[1] Present address: Daihatsu Co. Ltd., Osaka, Japan.

[2] Present address: Kyosera-Mita Co. Ltd., Osaka, Japan.

0022-460X/03/$ - see front matter
doi:10.1016/S0022-460X(02)01407-4

1. Introduction

The horn-type loudspeaker consists of an electrodynamic driver, a plate or shell diaphragm with elastic suspension and a radiation horn [1]. It has an axisymmetric configuration in many cases, whose typical cross-section is depicted in Fig. 1. The high-fidelity reproduction requires less distortion, which is mainly caused from the magnetic non-linearity of the york, the uneven magnetic field distribution between the poles, the non-linear behavior of the suspension system and the high sound intensity and velocity in the acoustic horn. The driver non-linearities have been modelled and studied [2,3].

The horn is an acoustic impedance matching transformer to increase the radiation efficiency. To provide smooth matching, it consists of a long duct with variable cross-section, which is in most cases folded as depicted to shorten the length. In the horn, the cross-section is very narrow in the throat and the bent regions, at which the sound may reach very high pressure and velocity. The high pressure and velocity cause the non-linear phenomena. Although there are many literatures on non-linear sound wave propagation [4–6] only within the scope of the one-dimension, there are few papers on the fields with arbitrary boundary shape or on heterogeneous media. The finite element approach was applied to the design of the horn speaker, a tweeter for the high-frequency range, in which no non-linear effects were considered [7]. The non-linear effects are included by the authors for the focused sound field problems in ultrasonic range [8,9], in which the finite element analysis was verified by the experiments [10,11]. The non-linear wave propagation has also been investigated for the horns [12–14]. Though some take the numerical approach, they exclude the driver's non-linearities.

In the present paper, the axisymmetric finite element formulation is made for a coupled magneto-mechano-acoustic system in time domain. In the formulation the magnetic non-linearity of the york and the acoustic non-linearity of the air are both included. In the following discussions, we confine ourselves to the simulation of the wave distortion and the harmonics generation based on the equation with relatively weak non-linearity. Though high velocity is known to cause some turbulence at discontinuities in the folds [15,16] and this effect cannot be ignored, this could not be included in the present formulation.

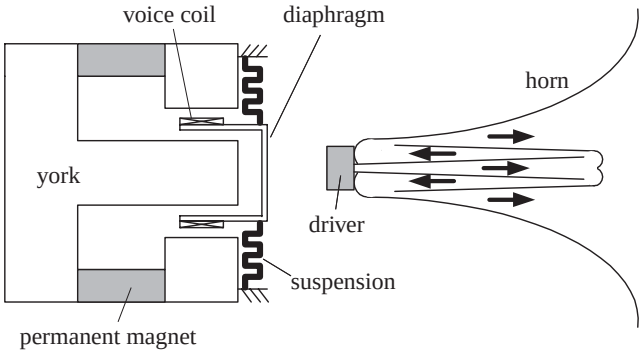

Fig. 1. A horn-speaker system.

2. Modelling

2.1. Non-linear sound field

The wave equation for sound field problems can be derived from the fluid dynamics equations. There are many possible expressions for non-linear waves depending on the degree of the non-linearity and the pressure–density relation to be included. After some manipulations, we arrive at the following expression for the velocity potential ϕ:

$$\left(1+\frac{\sigma}{c_0^2}\frac{\partial}{\partial t}\right)\nabla^2\phi-\frac{1}{c_0^2}\frac{\partial^2\phi}{\partial t^2}=-\frac{1}{c_0^2}\frac{\partial}{\partial t}\left[(\nabla\phi)^2+\frac{1}{2c_0^2}\frac{B}{A}\left(\frac{\partial\phi}{\partial t}\right)^2\right] \tag{1}$$

which is known as Kuznezov's equation [17], where c_0 is the sound speed, σ is the diffusion constant, $A=\rho_0 c_0^2/P_0, B=(c_0^2/P_0)(\partial^2 p/\partial\rho^2)_0$, ρ is medium density and P_0 is ambient pressure. The equation is expressed for the sound pressure p as

$$\begin{aligned}\left(1+\frac{\sigma}{c_0^2}\frac{\partial}{\partial t}\right)\nabla^2 p-\frac{1}{c_0^2}\frac{\partial^2 p}{\partial t^2}&=-\frac{\gamma}{\rho c_0^4}\frac{\partial^2 p^2}{\partial t^2}\\&=-\frac{2\gamma}{\rho c_0^4}\left[\left(\frac{\partial p}{\partial t}\right)^2+p\frac{\partial^2 p}{\partial t^2}\right]\end{aligned} \tag{2}$$

which is known as Westervelt's equation [18], under the assumption that the waves propagate locally in plane ($p=\rho c_0 v$), where

$$\gamma=1+\frac{B}{2A} \tag{3}$$

and ρ is the density of the medium and v is the particle velocity.

Eq. (2) can alternatively be written in the form of the standard wave equation with variable sound speed

$$\nabla^2 p-\frac{1}{c_n^2}\frac{\partial^2 p}{\partial t^2}=0, \tag{4}$$

where

$$c_n=\left(1+\frac{\gamma p}{\rho c_0^2}\right)c_0. \tag{5}$$

This expression is obtained from Eq. (2) for $\sigma=0$ and $\gamma p/(\rho c_0^2)\ll 1$. This shows that the sound speed depends on the pressure in which the wave travels faster in higher pressure level.

When the velocity potential consists of the primary wave ϕ_1 and the secondary wave ϕ_2 so that $\phi=\phi_1+\phi_2$, Eq. (1) can be decoupled under the assumption of weak non-linearity to give

$$\nabla^2\phi_1-\frac{1}{c_0^2}\frac{\partial^2\phi_1}{\partial t^2}=0, \tag{6}$$

$$\nabla^2\phi_2-\frac{1}{c_0^2}\frac{\partial^2\phi_2}{\partial t^2}=-\frac{1}{c_0^2}\frac{\partial}{\partial t}\left[(\nabla\phi_1)^2+\frac{1}{2c_0^2}\frac{B}{A}\left(\frac{\partial\phi_1}{\partial t}\right)^2\right]. \tag{7}$$

With the plane wave impedance relation, Eq. (7) can be written as

$$\nabla^2\phi_2 - \frac{1}{c_0^2}\frac{\partial^2\phi_2}{\partial t^2} = -\frac{\gamma}{c_0^4}\frac{\partial}{\partial t}\left(\frac{\partial\phi_1}{\partial t}\right)^2. \tag{8}$$

The driving term of Eqs. (7) and (8) comes from the contribution of the primary waves ϕ_1.

2.2. Electromagnetic field and driving force

The equation for the electromagnetic field in the driver can be derived from Maxwell's equations. The governing equation for the field without the displacement current and charge is expressed as follows when the eddy current and the induction current are ignored [19]:

$$\nabla \times (v\nabla \times \mathbf{A}) = \mathbf{J}_v + \mathbf{J}_m, \tag{9}$$

where v is the magnetic reluctance, $\mathbf{A}$ is the magnetic vector potential ($\mathbf{B} = \nabla \times \mathbf{A}, \mathbf{B}$ is the magnetic flux), $\mathbf{J}_v$ is the source current density in the voice coil and $\mathbf{J}_m$ is the equivalent magnetizing current density due to the permanent magnet ($\mathbf{J}_m = v_0\nabla \times \mathbf{M}, \mathbf{M}$: magnetization, v_0: the magnetic reluctance in the vacuum).

Electromagnetic (repulsive) force $\mathbf{F}_m$ acting between the pole and the voice coil when the electromagnetic induction due to the motion of the voice coil is neglected is given as

$$\mathbf{F}_m = \int_\Omega \mathbf{J}_v \times \mathbf{B}\,\mathrm{d}\Omega, \tag{10}$$

where Ω indicates the region in which the exciting current exists. This is the driving force for the elastic plate or the diaphragm.

2.3. Diaphragm and suspension

For mechanical motion of the diaphragm and the suspension, the constitutive relation or the stress–strain relation and the equation of motion are, respectively, defined as

$$\mathbf{T} = \mathbf{cS}, \tag{11}$$

$$\mathbf{F} = \rho\ddot{\mathbf{u}}, \tag{12}$$

where $\mathbf{T}, \mathbf{S}$ and $\mathbf{c}$ are, respectively, stress, strain and stiffness tensors, and $\mathbf{u}, \mathbf{F}$ and ρ are the displacement, the force vector and the mass density. In the elastic material used, the stress–strain relation (11) is assumed to be linear.

3. Finite element discretization

3.1. Acoustic radiation

We here discuss the solution of Eq. (2) for the axisymmetric case, which is discretized based on the Galerkin method. For the finite element discretization, triangular ring elements of the first

order are used throughout this paper. The discretized equation has the form [8,11,20]

$$[M_a]\{p\} + [R_a]\{\dot{p}\} + [K_a]\{\ddot{p}\} = \{a\} + (\{\dot{p}\}\{\dot{p}\}^{\mathrm{T}} + \{p\}\{\ddot{p}\}^{\mathrm{T}})\{W_n\} \tag{13}$$

when the system is driven by a rigid piston with the acceleration $\{a\}$ in which the second term in the driving term is due to the sound non-linearity. $[M_a], [K_a]$ and $[R_a]$ are an inertance, elastance and damping matrix, $\{p\}$ and $\{W_n\}$ are the nodal pressure and distribution vector, respectively, and the dot indicates the derivation with respect to time. The Newmark-β method [21] is used for the solution of time-marching. The calculation procedure can be given as

$$\begin{aligned}[M_a]\{p_{t+\Delta t}\} + [R_a]\{\dot{p}_{t+\Delta t}\} + [K_a]\{\ddot{p}_{t+\Delta t}\} \\ = \{a_{t+\Delta t}\} + (\{\dot{p}_{t+\Delta t}\}\{\dot{p}_{t+\Delta t}\}^{\mathrm{T}} + \{p_{t+\Delta t}\}\{\ddot{p}_{t+\Delta t}\}^{\mathrm{T}})\{W_n\},\end{aligned} \tag{14}$$

$$\{p_{t+\Delta t}\} = \{p_t\} + \Delta t\{\dot{p}_t\} + (\Delta t)^2[(0.5-\beta)\{\ddot{p}_t\} + \beta\{\ddot{p}_{t+\Delta t}\}], \tag{15}$$

$$\{\dot{p}_{t+\Delta t}\} = \{\dot{p}_t\} + \Delta t[(0.5-\eta)\{\ddot{p}_t\} + (1+\eta)\{\ddot{p}_{t+\Delta t}\}], \tag{16}$$

where Δt is a time step, β is a parameter for the time-marching and $\eta(\geqslant 0)$ is the artificial viscosity [22], which is sometimes introduced for the stable calculation with the shock wave, here $\eta = 0.06$ is chosen. In the present modelling, β is chosen to be 0.25 after some numerical experiments.

3.2. Magnetic field

The discretized equation corresponding to Eq. (9) is given as

$$[S]\{A\} = \{J_v\} + \{J_m\}, \tag{17}$$

where $[S]$ is the system matrix for the magnetic field and $\{A\}, \{J_v\}$ and $\{J_m\}$ are the nodal vectors of the magnetic vector potential, the exciting current of the voice coil and the equivalent current of the magnetization corresponding to the permanent magnet, respectively.

The york of the driver has a non-linearity in which the magnetic reluctance is a function of the square of the magnetic flux or the vector potential so that the discretized equation (17) is non-linear. The Newton–Raphson method is applied for the solution of the non-linear equation in which the solution can be obtained iteratively starting from a certain initial distribution of the magnetic vector potential $\{A\}^{(0)}$ [23]. The approximate solution of the $i+1$th iteration is corrected from the ith approximate solution as

$$\{A\}^{(i+1)} = \{A\}^{(i)} + \{\delta A\}, \tag{18}$$

where $\{\delta A\}$ is the increment of the vector potential which is obtained by the solution of the following equation:

$$\begin{bmatrix} \dfrac{\partial G_1}{\partial A_1} & \cdots & \dfrac{\partial G_1}{\partial A_N} \\ \vdots & & \vdots \\ \dfrac{\partial G_N}{\partial A_1} & \cdots & \dfrac{\partial G_N}{\partial A_N} \end{bmatrix} \{\delta A\} = -\{G\}, \tag{19}$$

where

$$\{G\} = [S]\{A\} - \{J_v\} - \{J_m\}. \tag{20}$$

Eqs. (18) and (19) are iteratively calculated until the convergence is reached in which the criterion is chosen to be

$$\frac{1}{N}\sum_{j=1}^{N}\left|\frac{A_j^{(i+1)} - A_j^{(i)}}{A_j^{(i+1)}}\right| < \varepsilon, \tag{21}$$

where ε is the small value for the criterion and N is the number of the nodes.

The discretized expression corresponding to the electromagnetic force (10) is given as [11,19]

$$\{F_m\} = \{J_v\}\{A\}^{\mathrm{T}}\{W_f\}, \tag{22}$$

where $\{F_m\}$ is the nodal electromagnetic force vector and $\{W_f\}$ is a distribution vector.

3.3. Elastic vibration

The discretized equation of the elastic vibration of the diaphragm is given by [11,24]

$$[K_m]\{d\} + [R_m]\{\dot{d}\} + [M_m]\{\ddot{d}\} = \{F\}, \tag{23}$$

where $[K_m], [R_m]$ and $[M_m]$ are the stiffness, damping and mass matrices, respectively, $\{d\}$ is the nodal displacement vector and $\{F\}$ is the nodal force vector due to the force externally applied. When the mechano-acoustic coupling is considered, $\{F\}$ in Eq. (23) and $\{a\}$ in Eq. (13) are, respectively, in the relation of

$$\{F\} = \{F_m\} - [W_a]\{p\}, \tag{24}$$

$$\{a\} = [W_a]^{\mathrm{T}}\{\ddot{d}\}, \tag{25}$$

where $[W_a]$ is the mechano-acoustic coupling matrix. The second term on the right-hand side of Eq. (24) corresponds to the force reacting from the sound pressure in the acoustic medium. The Newmark-β method is again used for the time-marching of Eq. (23). The calculation procedure is the same as Eqs. (14)–(16).

4. Numerical examples

4.1. Acoustic field

First we discuss the validity of the solution procedure. The evaluation is made for a one-dimensional tube as shown in Fig. 2. The length of the pipe is 50λ where λ is the wavelength of the excitation sinusoidal wave, and the radius is 0.1λ. The pipe is driven at one end ($z = 0$) by the uniform velocity and at another end ($z = \ell$) it is terminated by the sound absorber with the surface acoustic impedance ρc_0. Other wall boundary is assumed to be rigid. The medium is assumed to be air ($\rho = 1.2$ kg/m^3, $c_0 = 340$ m/s and $\gamma = 1.2$). The solutions are shown in Fig. 3, when one-cycle of the sine wave excites the system. The waveforms distort as they propagate and a shock finally develops. It is seen that the solution is not stable without proper artificial viscosity [22]. The FEM

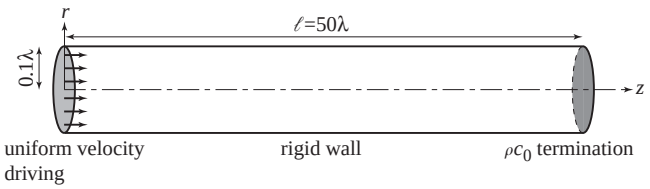

Fig. 2. A one-dimensional tube.

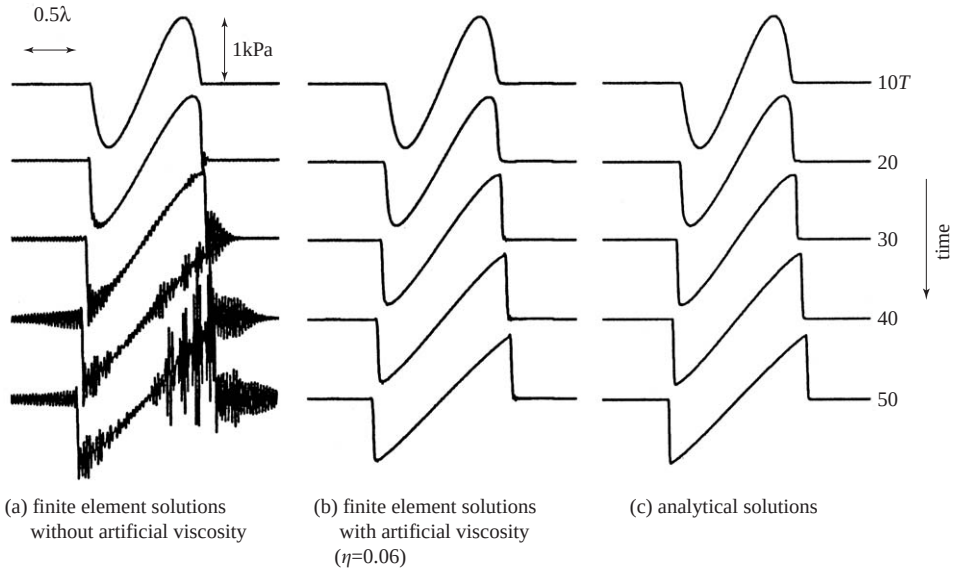

Fig. 3. Pressure waveform evolution for plane wave in air for one-cycle of sinusoidal excitation ($P = 1$ kPa, $\Delta\ell = \lambda/70$).

solutions with the artificial viscosity agree well with the analytical solutions. We are now confident that the non-linear sound propagation can thus be simulated with reasonable accuracy by FEM.

The non-linear sound wave propagation from the circular rigid piston as shown in Fig. 4 is then demonstrated. A circular piston with the radius of 1λ is uniformly driven by the sinusoidal wave for the one-cycle. The opening boundary is terminated by the ρc_0 characteristic impedance, which does not provide the perfectly absorbing termination but is convenient to treat the waves of the wide range of the spectra. The buffle board outside the piston and the central axis are assumed to be rigid. The non-linear sound propagation for the amplitude of 5 kPa is illustrated until the time $5T$ in Fig. 5. The solutions are compared with the solutions of the discrete Huygens' modelling [25]. The waveform is again distorted as it propagates until weak shock develops.

4.2. Response of the horn with a driving unit

The response of the loudspeaker horn is then demonstrated. The cross-section views and their element divisions are illustrated in Fig. 6. The permanent magnet in the driver unit is equivalent to

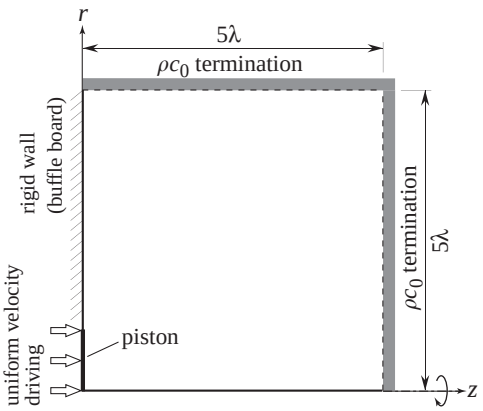

Fig. 4. An axisymmetric field and a circular piston.

the electromagnet supplied by the direct current of the amplitude of 1×10^6 A/m^2. The voice coil is excited by the starting-up sinusoidal current with the peak amplitude of 4×10^7 A/m^2 as shown in Fig. 7. The magnetic characteristics of the york and the magnet are shown in Fig. 8, which are both non-linear. The magnetic boundary condition on the z-axis is assumed to be $A_\theta = 0$ and the r axis is assumed to be of natural boundary. The hybrid-type infinite elements are connected for outer magnetic boundary [23]. For the diaphragm and the suspension, their mechanical material constants used in the calculation are tabulated in Table 1. The edge of the suspension of the opposite side of the diaphragm is assumed to be fixed. The displacement in the r direction u_r is assumed to be $u_r = 0$ on the central z-axis. The horn is terminated out of the opening by the ρc_0 characteristic impedance. This is convenient for the present problem with the wide range of frequency spectra involved, though the treatment does not provide the perfectly absorbing termination. In the horn loudspeaker considered [7], the radiation field was expressed being expanded in terms of the Bessel function.

The displacement in the z direction at the center of the diaphragm is shown in Fig. 9 when the voice coil is excited by the sinusoidal current of frequency $f = 1300$ Hz. The building-up waveform is almost identical to that of the exciting current of the voice coil except with a little fluctuation, which will be explained later. In this case, the time step is chosen to be $\Delta t = 3.846$ μs. Fig. 10 illustrates the motion of the displacement of the diaphragm when the response has reached the steady state. The diaphragm moves just like a piston. Fig. 11 shows the equi-pressure lines of the wavefront of the sound marching in the horn when the sinusoidal wave of frequency $f =$ 1300 Hz is turned on. Fig. 12 shows the sound pressure response at the center of the horn opening. A building-up waveform is similar to that of the exciting current but distorted. The delayed response corresponds to the propagation time to the horn opening. Fig. 13 shows the Fourier transformed frequency characteristics of the sound pressure. In the figure, the dashed and the fine lines, respectively, indicate the characteristics when the magnetic and the acoustic non-linearities are separately considered, and the bold line when magnetic and acoustic non-linearities are both included. The second harmonic (f_2), double of the frequency, is resulting from the non-linearities. All the responses are similar except this peak, which is very dominated when the acoustic non-linearity is included. The peak lower than fundamental frequency (f_1) is due to the resonance of

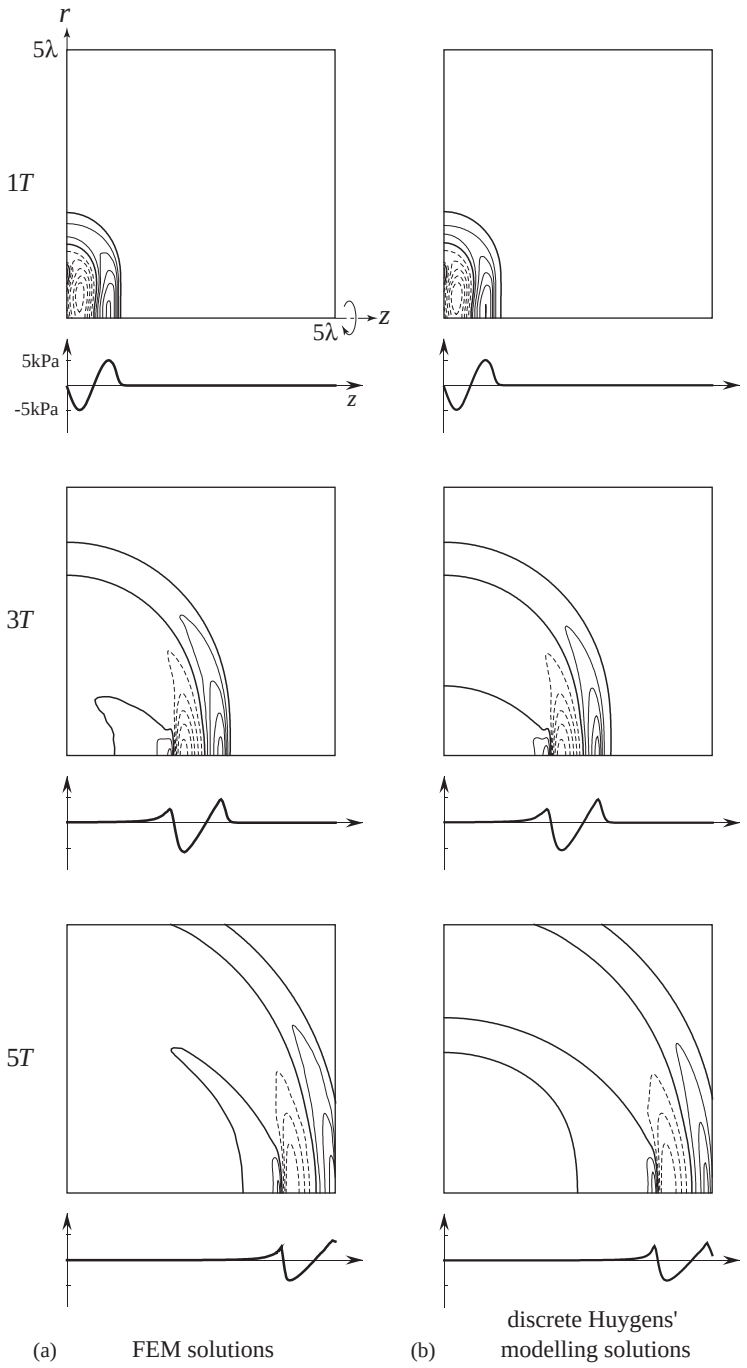

Fig. 5. Non-linear wave propagation for a one-cycle sinusoidal wave in axisymmetric field ($P = 5$ kPa, $\Delta\ell = \lambda/40$).

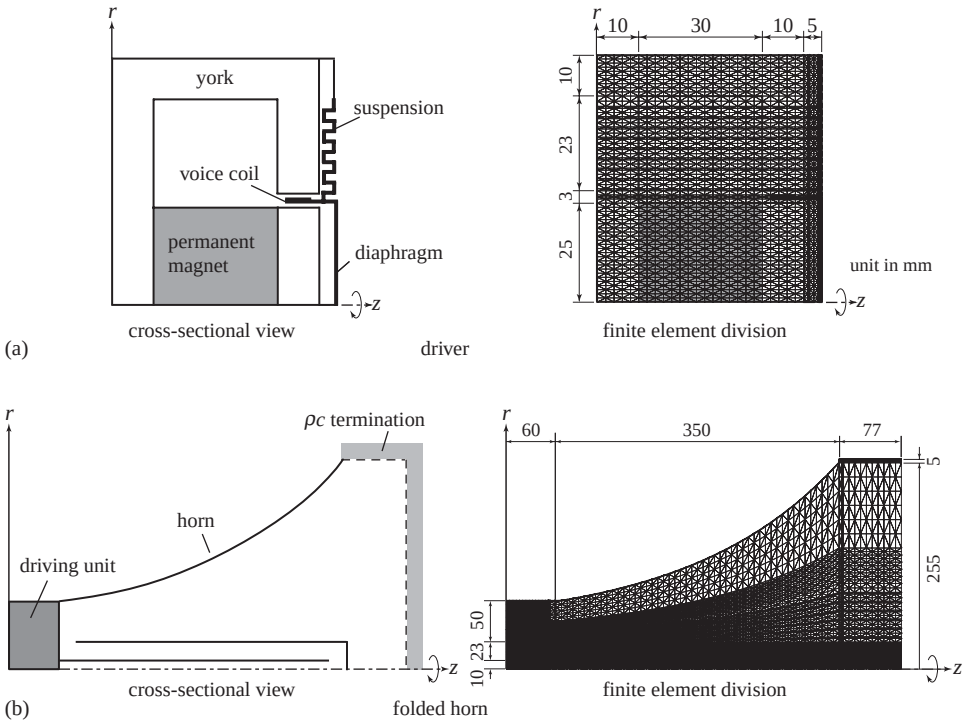

Fig. 6. Cross-section view of a loudspeaker horn.

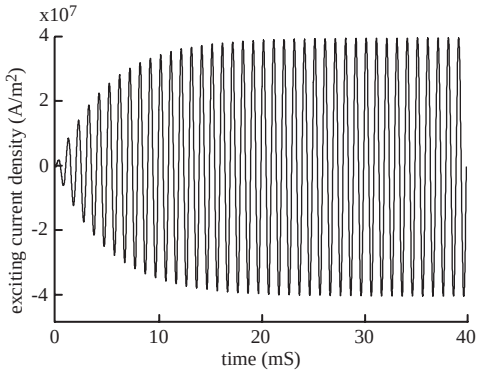

Fig. 7. Exciting current supplied to the voice coil.

the diaphragm-suspension system without acoustic loading (so-called f_0) as shown in Fig. 14. Other small peaks come from the non-linear cross coupling between the peaks. Fig. 15 shows the second harmonic distortion resulting from each non-linearity when the amplitude of the exciting current is varied at frequency $f = 1300$ Hz. In the figure, the distortion is expressed as the sound pressure level of the second harmonic against the fundamental. The distortion resulting from the

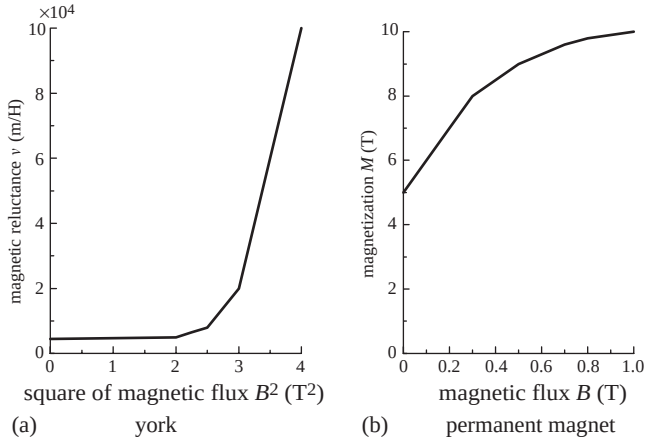

Fig. 8. Magnetic characteristics of the york and the magnet.

Table 1
Material constants used in the calculation

	Diaphragm	Voice coil	Suspension
Density (kg/m^3)	2700	8900	500
Young's modulus ($\times 10^{10}$ Pa)	7.1	12.2	1
Poisson's ratio	0.33	0.35	0.3

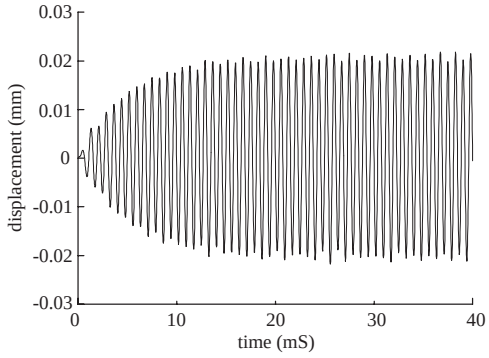

Fig. 9. Displacement at the center of the diaphragm.

acoustic non-linearity increases almost in proportion to the exciting current density. In this case the acoustic non-linearity is predominant. The frequency characteristics of the horn at the center of its opening is shown in Figs. 16 and 17. This is taken when the responses have reached the steady states of excitation at each frequency. The irregularity is due to the reflections at the foldings and the opening in the horn. Fig. 16 shows the generation of the modulated distortion

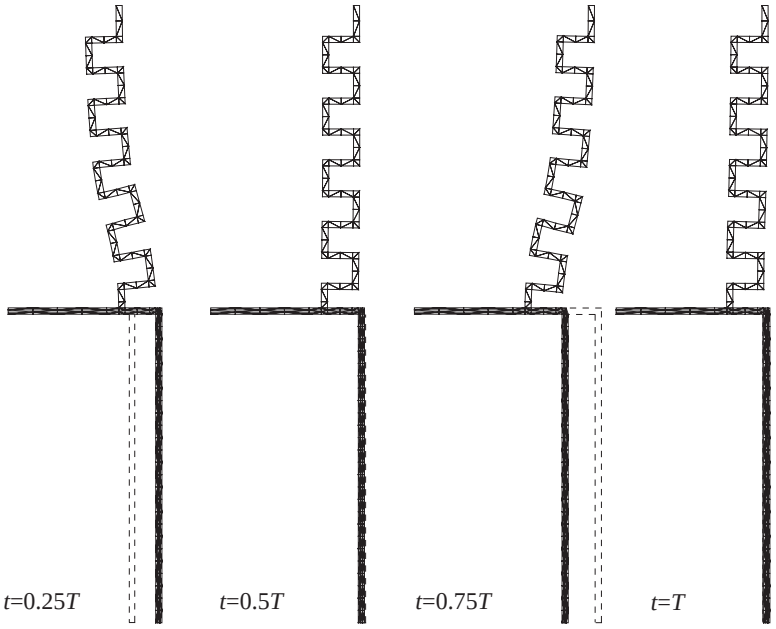

Fig. 10. Motion of the displacement of the diaphragm.

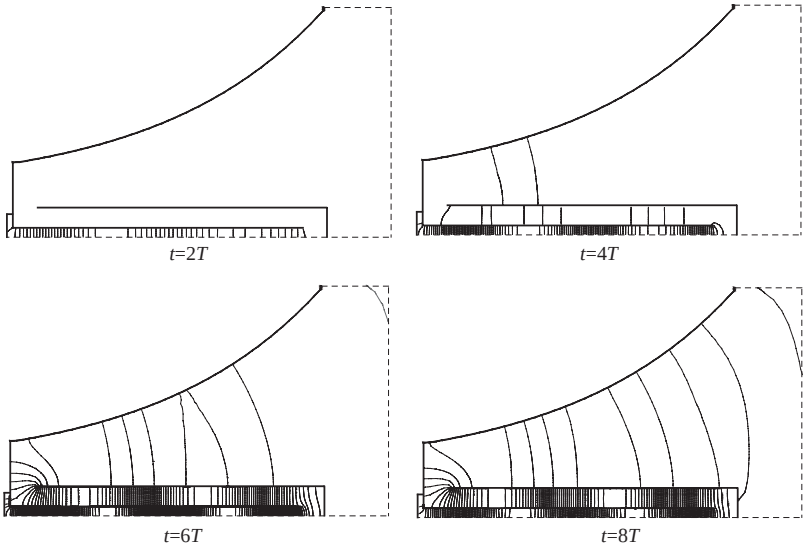

Fig. 11. Marching of the sound (equi-pressure lines).

when sound waves of $f_\ell = 100$ Hz and $f_h = 1300$ Hz are both simultaneously excited. The high-frequency wave f_h is modulated by the low-frequency wave f_ℓ. In this case the modulation indexes for f_h and $2f_h$ are about 12% and 23%. The second harmonic $2f_h$ is modulated twice as much.

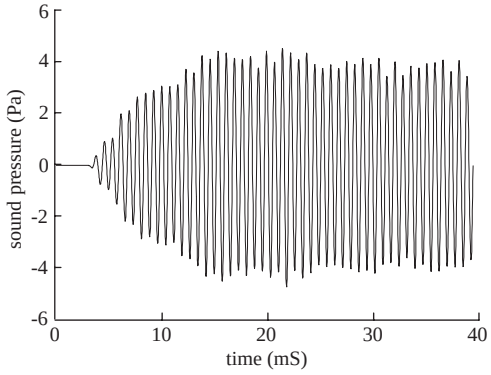

Fig. 12. Sound pressure waveform at the center of the horn opening.

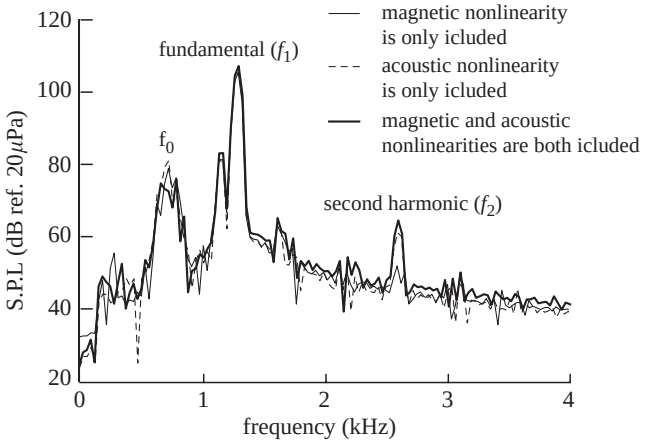

Fig. 13. Fourier transformed frequency characteristics of the sound pressure.

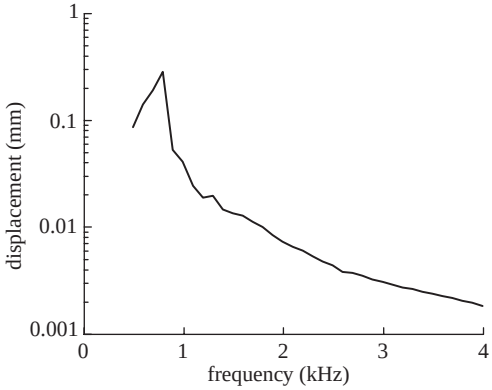

Fig. 14. Frequency characteristics of the diaphragm-suspension system.

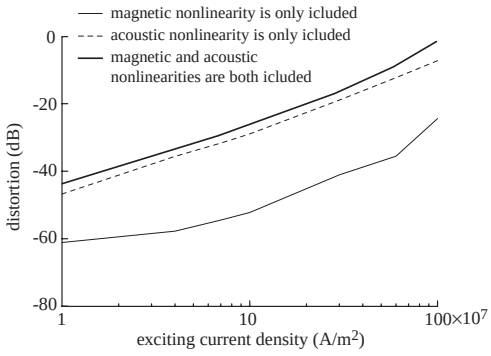

Fig. 15. Second harmonic distortion.

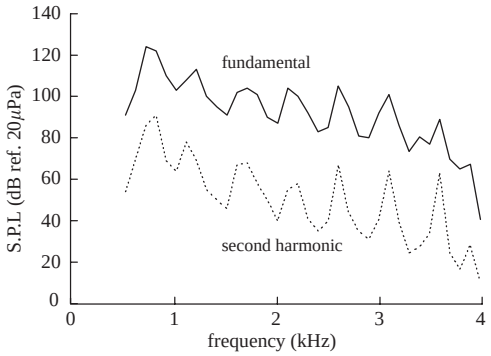

Fig. 16. Frequency characteristics.

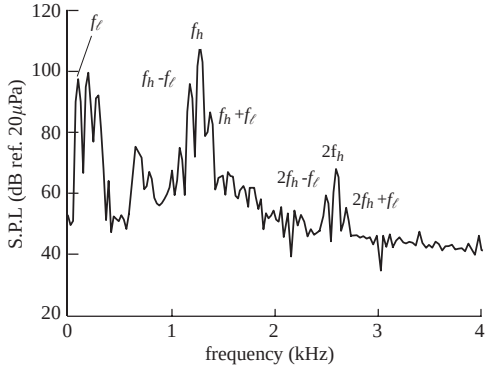

Fig. 17. Modulation distortion, $f_\ell = 100$ Hz and $f_h = 1300$ Hz.

5. Concluding remarks

The finite element technique is applied to simulating the dynamic response of the horn loudspeaker with the non-linearity included. The axisymmetric finite element formulation is

developed for a coupled magneto-mechano-acoustic system. The magnetic non-linearity resulting from the B^2–v curve of the york in the driver which is solved by Newton–Raphson method and the acoustic non-linearity of the medium are both included in the formulation. The discretized simultaneous equations are solved by Newmark-β integration scheme with respect to time. Some numerical examples are demonstrated for predicting the sound radiation characteristic of the loudspeaker. It is shown that the distortion in the horn resulting from the acoustic non-linearity is largest among others. The finite element simulation provides a good guideline to the loudspeaker horn design.

The work has partly been reported at 19th Computational Electromagnetics and Electronics, Japan Society for Simulation Technology, 1998 [19] and at 7th International Conference on Sound and Vibration, 2000 [26].

References

[1] H.F. Olson, Elements of Acoustical Engineering, 3rd edition, Van Nostrand, New York, 1957.
[2] W. Klippel, Modeling the non-linearities in horn loudspeakers, Journal of the Audio Engineering Society 44 (6) (1996) 470–480.
[3] W. Klippel, Nonlinear system identification for horn loudspeakers, Journal of the Audio Engineering Society 44 (10) (1996) 811–820.
[4] O.V. Rudenko, S.I. Soluyan, Theoretical Foundations of Nonlinear Acoustics, Studies in Soviet Science, Consultants Bureau, Plenum, New York, 1977.
[5] T. Kamakura, Fundamentals of Nonlinear Acoustics, Aichi, Tokyo, 1996.
[6] M.F. Hamilton, D.T. Blackstock, Nonlinear Acoustics, Academic, San Diego, CA, 1998.
[7] N. Kyono, S. Sakai, S. Morita, Y. Kagawa, Acoustic radiation of a horn loudspeaker by the finite element method—acoustic characteristics of horn loudspeaker with an elastic diaphragm, Journal of the Audio Engineering Society 30 (12) (1982) 896–905.
[8] T. Tsuchiya, Y. Kagawa, Finite element analysis of focusing field in non-linear acoustic waves, Japan Journal of Applied Physics 30 (Suppl. 30-1) (1991) 51–53.
[9] Y. Kagawa, T. Tsuchiya, T. Yamabuchi, H. Kawabe, T. Fujii, Finite element simulation of non-linear sound wave propagation, Journal of Sound and Vibration 154 (1) (1992) 125–145.
[10] T. Tsuchiya, Y. Kagawa, Finite element analysis of non-linear sound field of a focusing source with large aperture angle, Journal of the Acoustical Society of Japan 49 (5) (1993) 334–339.
[11] T. Tsuchiya, Y. Kagawa, T. Okamuro, Y. Mashima, Finite element simulation of electromagnetic induction transducers for impulsive intense sound, IEEE Transactions on Ultrasonics, Ferroelectrics and Frequency Control 44 (5) (1997) 1077–1086.
[12] W. Klippel, Nonlinear wave propagation in horns and ducts, Journal of the Acoustical Society of America 98 (1995) 431–436.
[13] K.R. Holland, C.L. Morfey, A model of non-linear wave propagation in horns, Journal of the Audio Engineering Society 44 (7/8) (1996) 569–580.
[14] P. Bequin, C.L. Morfey, Weak non-linear propagation of sound in a finite exponential horns, Journal of the Acoustical Society of America 109 (6) (2001) 2649–2659.
[15] B. Roozen, M. Bockholts, P. van Eck, M. Hirschberg, Vortex sound in bass-reflex ports of loudspeakers, Part I & II, Journal of the Acoustical Society of America 104 (1998) 1914–1924.
[16] A. Salvatti, A. Devantier, D.J. Button, Maximizing performance from loudspeaker ports, Journal of the Audio Engineering Society 50 (1/2) (2002) 19–45.
[17] V.P. Kuznetsov, Equations of nonlinear acoustics, Soviet Physics Acoustics 16 (1971) 467–470.
[18] P.J. Westervelt, Parametric acoustic array, Journal of the Acoustical Society of America 35 (1963) 535–537.

[19] M. Doi, T. Tsuchiya, Y. Kagawa, Finite element simulation of a horn type dynamic speaker, 19th Computational Electromagnetics and Electronics, JSST 1-I-5 (1998) 37–40.
[20] Y. Mino, T. Tsuchiya, Y. Kagawa, Finite element simulation of non-linear sound distortion—on waveform distortion radiated from a horn speaker, 18th Computational Electromagnetics and Electronics, JSST 2-II-3 (1997) 209–212.
[21] N.M. Newmark, A method of computation for structural dynamics, Proceedings of American Society of Civil Engineers, Journal of Engineering Mechanics Division 85-EM3 (1959) 67–94.
[22] T. Tsuchiya, Y. Kagawa, A simulation study on non-linear sound propagation by finite element approach, Journal of the Acoustical Society of Japan (E) 13 (4) (1997) 223–230.
[23] Y. Kagawa, T. Murai, Finite element simulation of magnetic recording-reproduction process with special attention to AC-biased recording mechanism, IEEE Transactions on Magnetics 26 (2) (1997) 987–990.
[24] O.C. Zienkiewitcz, The Finite Element Method, McGraw-Hill, New York, 1977.
[25] Y. Kagawa, T. Tsuchiya, B. Fujii, K. Fujioka, Discrete Huygens' model approach to sound wave propagation, Journal of Sound and Vibration 218 (3) (1998) 419–444.
[26] Y. Kagawa, T. Tsuchiya, M. Doi, T. Tsuji, Finite element simulation of a loudspeaker horn characteristics—numerical solution of nonlinear acoustic waves with the applications, Proceedings of Seventh International Conference on Sound and Vibration, Vol. IV, 2000, pp. 2203–2210.